IEEE Access
Multidisciplinary | Rapid Review | Open Access Journal

Received May 5, 2019, accepted June 10, 2019, date of publication June 26, 2019, date of current version September 9, 2019.

Digital Object Identifier 10.1109/ACCESS.2019.2925000

Design of Compact Rotman Lens Using Truncated Ports With Energy Distribution Slots

QIUYAN LIANG[1], BAOHUA SUN[1], GAONAN ZHOU[1], JIANPING ZHAO[2], AND GUANXI ZHANG[3]

[1]National Key Laboratory of Antennas and Microwave Technology, Xidian University, Xi'an 710071, China
[2]Antenna and System Technology Centre, Huawei Technologies Company Ltd., Shanghai 200120, China
[3]System Technology Research Department, WN [Carrier Network BG], Huawei Technologies Company Ltd., Shanghai 201206, China

Corresponding author: Baohua Sun (bhsun@mail.xidian.edu.cn)

ABSTRACT A compact Rotman lens is presented in this paper. The compact Rotman lens consists of a lens body and truncated ports with the energy distribution slots. By truncating the long triangular transitions of the traditional Rotman lens, the lengths of lens ports are reduced effectively. However, the impedance discontinuity problem is caused by truncating the triangular transition. To solve this problem, the energy distribution slots are designed between the feed lines and the truncated lens body apertures. The energy distribution slot is evolved from the 1–2 power divider, which creates a transition process for the wave energy propagating from the feed lines and realizes good impedance match between the lens body and the feed lines. To validate the proposed design, a 4×7 Rotman lens has been designed and prototyped at 10 GHz. The Rotman lens exhibits a scanning range of $\pm 33°$, 27% bandwidth for VSWR < 2, and the isolation between beam ports better than 17.2 dB within the operation bandwidth. Basing on the advantages of compact size, low cost, easy processing, and wide bandwidth, the proposed compact Rotman lens may have wide applications in the multi-beam antenna systems.

INDEX TERMS Beam-former, compaction, lens port, low cost, Rotman lens.

I. INTRODUCTION

Passive beam-formers have received considerable attention with the expansion of wireless communications in the last several decades [1]–[3]. The Rotman lens is a conventional passive beam-former [4]. Due to its many advantages such as true time delay (TTD) characteristics, multi-beam capabilities, and wide bandwidth, it has been widely used in multi-beam antenna systems, such as commercial radars and base stations antenna systems.

Various structures of Rotman lens have been presented in literatures [5]–[7]. In [5], a Rotman lens using a graded dielectric substrate is presented to realize the insertion loss improvement. In [6], a defocused Rotman lens is presented to reduce the conjugate port coupling. In [7], an ultra-wideband scanning antenna array is realized by achieve the minimum phase-error of the Rotman lens. However, most conventional Rotman lenses have considerable large size, which causes difficulties on their integration with compact transceiver systems.

The associate editor coordinating the review of this manuscript and approving it for publication was Sandra Costanzo.

Some approaches have been proposed to reduce the occupied area of the Rotman lens. In [8], a two-layer Rotman lens-fed microstrip antenna array is proposed. The layout of lens body and the antennas are placed on different layers. In [9], the lens body of the Rotman lens is folded into two layers along its middle plane and coupling slots are used as transitions. Both of the methods in [8] and [9] reduce the occupied area of the Rotman lens compared to the single-layer implementations. However, the coupling slots between two layers have narrow bandwidth, which leads to the reduction of operation bandwidth of the Rotman lens. In [10], a multilayer substrate integrated waveguide (SIW) technology is used to fold the array ports of the Rotman lens and the broadband star-shaped coupling slots are used as transition, which constitute a compact multi-beam antenna system. Similarly, in [11], a slot array in SIW technology and a Rotman lens are designed on different layers. In [12], a wrapped Rotman lens is proposed to integrate with a mobile phone, which reduces the dimension of the Rotman lens. However, the SIW antenna system in [10], [11] needs complicate manufacturing processes and the wrapped Rotman lens in [12] needs special conformal expensive substrate, which

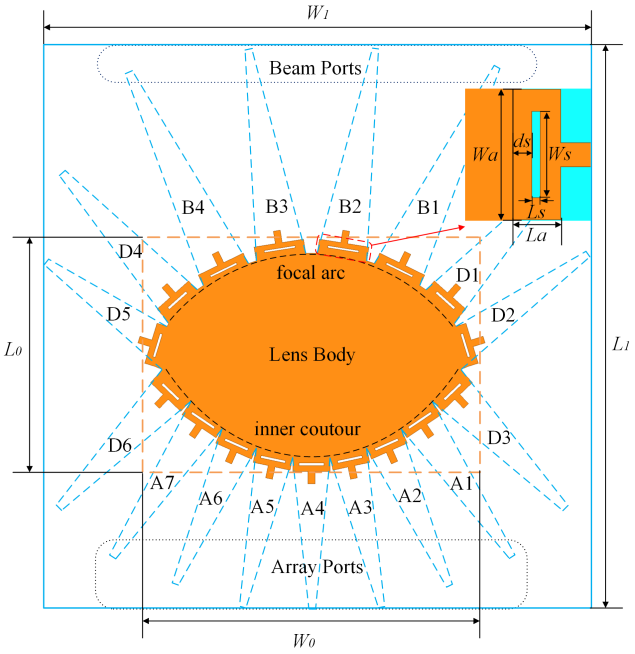

FIGURE 1. Layouts of Rotman lenses. $W0 = 4.8\lambda g$, $L0 = 3.3\lambda g$, $W1 = 7.8\lambda g$, $L1 = 8\lambda g$. (Blue dot line shows the layout of traditional Rotman lens.).

are not suitable for the massive civilian applications. Another approach to reduce the physical size of the Rotman lens is to use the dielectric substrates with high permittivity. But most of such substrates are expensive and also not suitable for the massive productions. All of these solutions reduce the physical size of the antenna system with Rotman lens to some extent, but it is noted that the processing area, which is equal to the total multilayer areas, is not reduced effectively. In conclusion, it is necessary to reduce the real total area of the Rotman lens without degrading its performance and increasing its cost of production.

The conventional Rotman lens consists of the lens body and lens ports marked with blue dot line as shown in Fig.1. The lens body is shaped of a focal arc and an inner lens contour. The port locations are designed basing on classical lens equations proposed by Rotman. The size of lens body is relatively constant to guarantee the phase relationship of the Rotman lens [13]. The conventional Rotman lens uses triangular transitions as the lens ports as shown in Fig.1. The triangular transition has been analyzed in [14] and [15] and the value of flare angle $\theta \leq 12.5°$ has been proven to be a reasonable value for triangular transition design, which leads to the large size of the lens ports.

One direct way of reducing the size of the Rotman lens is to truncate the long traditional triangular transitions. However, this will cause impedance discontinuity problem if the 50Ω feed line is connected to the lens body directly. In our previous work, a compact Rotman lens using Chebyshev impedance transformers has been proposed to reduce the size of the lens ports [16]. To further reduce the size of the lens ports, the truncated ports with energy distribution slots is proposed in this paper. The truncated port with energy distribution slot is evolved from 1-2 power divider. It can create the transition process for the wave energy propagating from the feed lines and realize good match between the lens body and feed lines. A 4×7 Rotman lens using truncated ports with energy distribution slots is designed and prototyped at 10GHz for the purpose of demonstration. The Rotman lens exhibits a good performance of return loss, insertion loss, and isolation.

The remainder of this paper is organized as follows. The structure of the compact Rotman lens is presented in Section II. The evolution process is described and analyzed in Section III. In section IV, the simulation and measurement results of the compact Rotman lens is provided. Finally, a summary and conclusions are given in Section V.

II. STRUCTURE OF COMPACT ROTMAN LENS

The layout of proposed compact Rotman lens is shown in Fig.1. The proposed Rotman lens consists of a lens body and truncated ports with energy distribution slots. The lens body is shaped of a focal arc and an inner lens contour. The lens contours and locations of ports are designed basing on the original Rotman lens design equations initially proposed by Rotman. The proposed Rotman lens has 4 beam ports B1-B4, 7 array ports A1-A7 and 6 dummy ports D1-D6. The beam ports are connected to the sources. The array ports are connected to the antenna array. The dummy ports are connected to the matched loads to absorb extra wave reflected from the lens body. When the beam port is excited, the wave from the beam port propagate through the lens body and arrive to the array ports. Due to the differences of the physical lengths from the excited beam port to every array port, a set of phase difference among array ports can be obtained and used to form the beam in certain direction. Here four sets of phase differences can be obtained to realize four beams when four beam ports are excited respectively.

From the Fig.1, the lens port is composed of short truncated port with rectangular energy distribution slot. The slot is located on the center line of each aperture and are bilateral symmetric. The existence of slot makes the truncated port into a structure with two transitions in parallel and finally connected to the feed lines. From Fig.1, It can be seen that the truncated ports with rectangular energy distribution slots have much shorter lengths than the traditional triangular transitions which are marked with blue dot line. By using the proposed lens ports, the occupied area of the 4 × 7 Rotman lens is reduced from $7.8\lambda g \times 8\lambda g$ to $4.8\lambda g \times 3.3\lambda g$, a considerable size reduction. From Fig.1, the area of lens body is nearly equal to the area of total compact Rotman lens.

The layout of the proposed Rotman lens is printed on the top metal layer of a substrate which is not shown in Fig.1. The substrate is Rogers RO4350 substrate with relative permittivity of 3.66, dielectric loss tangent of 0.004 and thickness of 30mil.

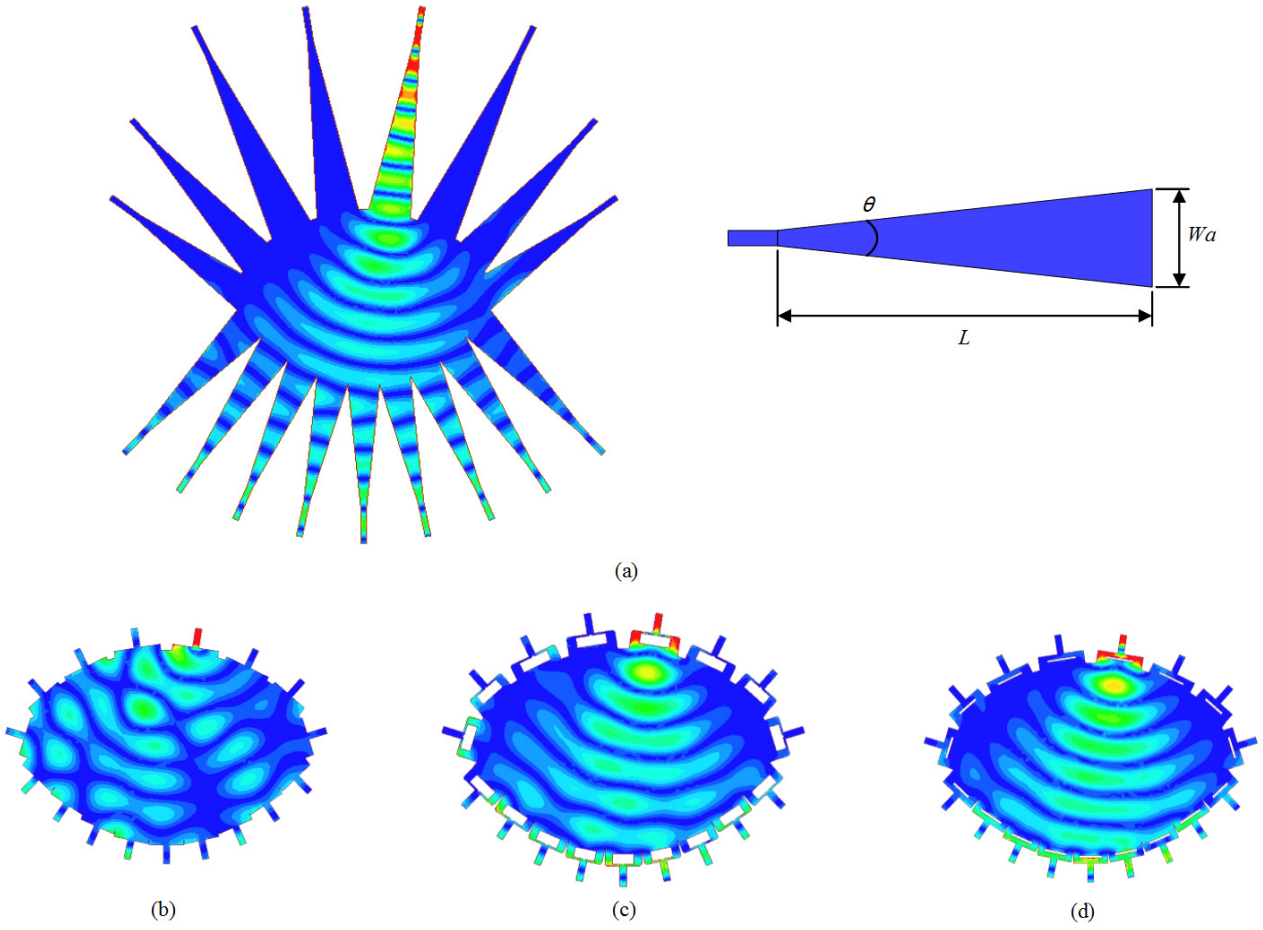

FIGURE 2. Current propagating across the lens with different ports (beam port B2 active). (a) Traditional triangular transitions and the triangular transitions, (b) Truncated ports, (c) Truncated ports with 1-2 power dividers, (d) Truncated ports with rectangular energy distribution slots.

III. EVOLUTION PROCESS AND ANALYSIS

In this section, the evolution process of the compact Rotman lens are presented. The evolution process of the compact Rotman lens can be separated to three steps. Fig.2 shows the steps of the evolution process of compact Rotman lens and the electric field simulations of their current propagating. From Fig.2, the 1-2 power dividers are connected to the lens ports after the triangular transitions are truncated. Then, the truncated ports with 1-2 power dividers evolve into the final truncated ports with rectangular energy distribution slots for further compacter layout. The detail discussions about the three steps are as follows.

A. STEP 1: TRUNCATE THE TRIANGULAR TRANSITIONS

Fig.2(a) is a traditional Rotman lens with triangular transitions. The flare angle of the triangular transitions is $\theta = 12.5°$ [14], the length of the triangular transition L can be calculated as follows:

$$L = \frac{\frac{W_a}{2}}{tan\frac{\theta}{2}} \approx 4.57W_a \tag{1}$$

where Wa is the width of the lens port aperture. From (1), it can be concluded that the triangular transition has considerable long length. Fig.2(b) is a Rotman lens with truncated ports. As can be seen from Fig.2(a) and Fig.2(b), truncating triangular transitions indeed reduces the total occupied area of the Rotman lens effectively. But it also can be observed that the wave energy from the 50Ω feed line cannot flow smoothly from the beam port to the array ports after truncating the lens port. It is because of that the width of lens port aperture is large but the width of 50Ω feed line is small. There is an impedance discontinuity problem when the 50Ω feed line is connected to the lens body directly.

B. STEP 2: CONNECT THE POWER DIVIDERS

To solve the impedance discontinuity problem, 1-2 power dividers are designed between the feed lines and the lens port apertures as shown in Fig.2(c). The 50Ω feed line is connected by two 100Ω transition lines in parallel. Then two 100Ω transition lines and two ends of lens port aperture are connected by two parallel transitions respectively. Here due to the irregular shape of the Rotman lens, the input impedance of the lens aperture is not easy to obtain, so the size parameters for parallel transitions are obtained by using the electromagnetic simulator ANSYS HFSS 15. By choosing suitable

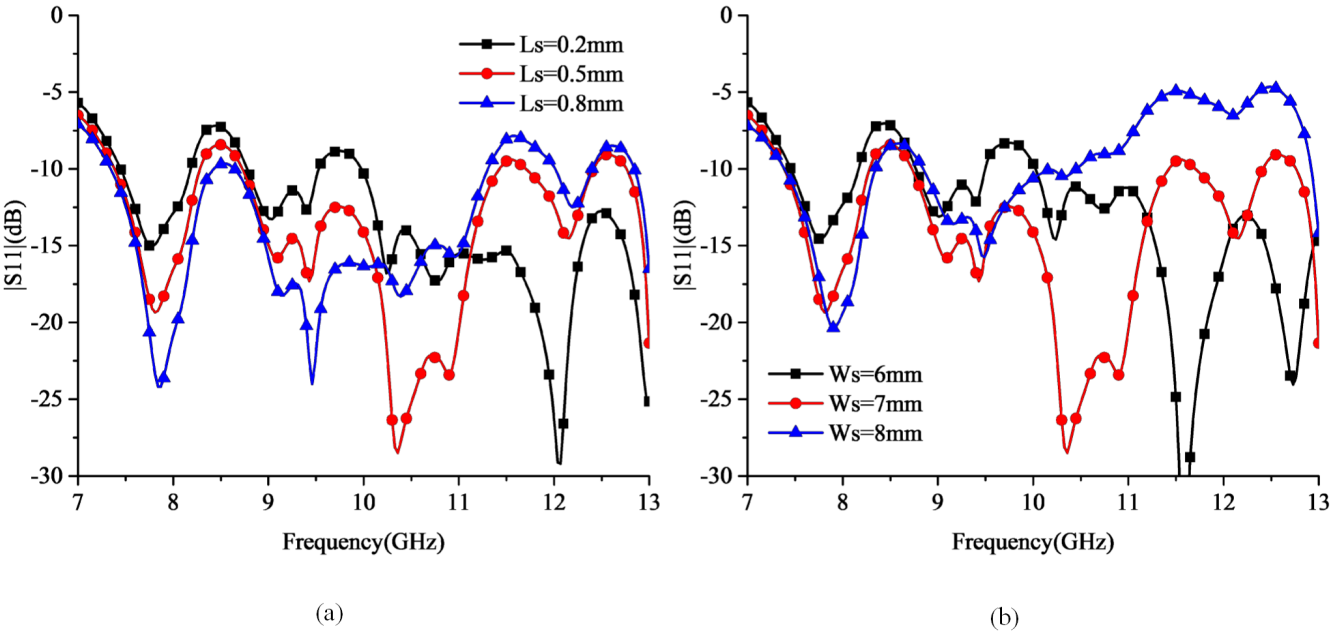

FIGURE 3. Results of |S11| for B2 of different slot parameters. (a) Different slot length *Ls*, (b) Different slot width *Ws*.

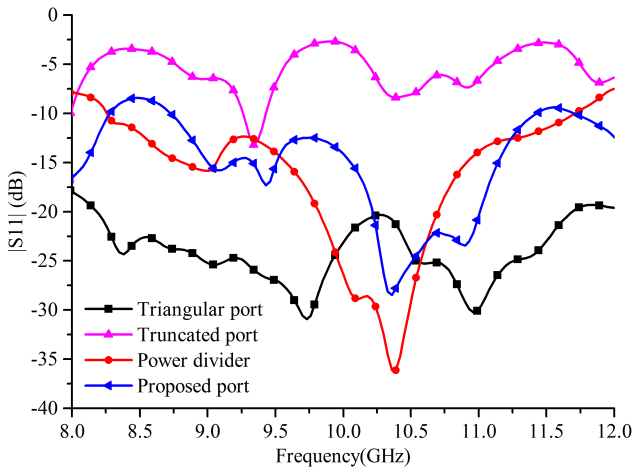

FIGURE 4. Results of |S11| for B2 of different Rotman lenses.

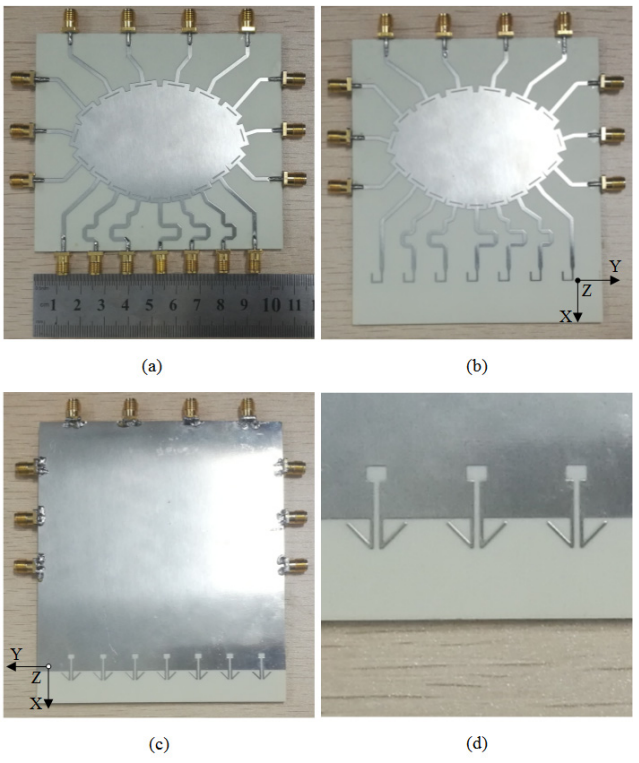

FIGURE 5. The prototypes of the Rotman lens. (a) Top view of Rotman lens, (b) Top view of Rotman lens combined with antenna array, (c) Bottom view of Rotman lens combined with antenna array, (d) Detail view of the antenna array.

size parameters for the parallel transitions, the impedance matching between lens port apertures and feed lines can be realized.

From the current propagating shown in Fig.2(c), the 1-2 power divider provides a transition process for the wave energy propagating from the feed lines. The wave energy from the 50Ω feed line propagates along two transitions and realizes in-phase stacking at the center of the lens body aperture due to the 1-2 power divider is symmetrical.

C. STEP3: SIMPLIFY POWER DIVERS TO SLOTS

To further simplify the design of the lens ports and reduce the size of the Rotman lens, the lens ports in step 2 evolve into the truncated ports with rectangular energy distribution slots as shown in Fig.2(d). The parameters of the energy distribution slots are also obtained by ANSYS HFSS 15.

To further investigate the effect of the slot parameters to the return losses of beam ports, the key design parameters are studied, such as the slot length *Ls* and slot width *Ws*. As shown in Fig.3, it is clear that the operation band shifts to

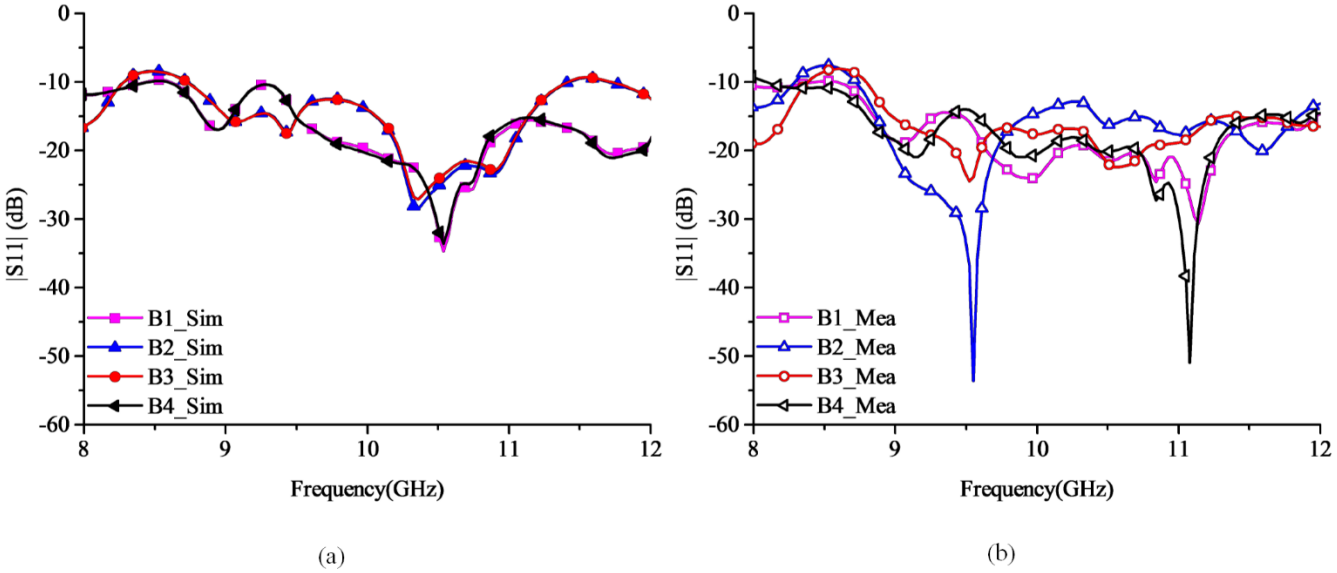

FIGURE 6. The results of |S11| of beam ports. (a) Simulations, (b) Measurements.

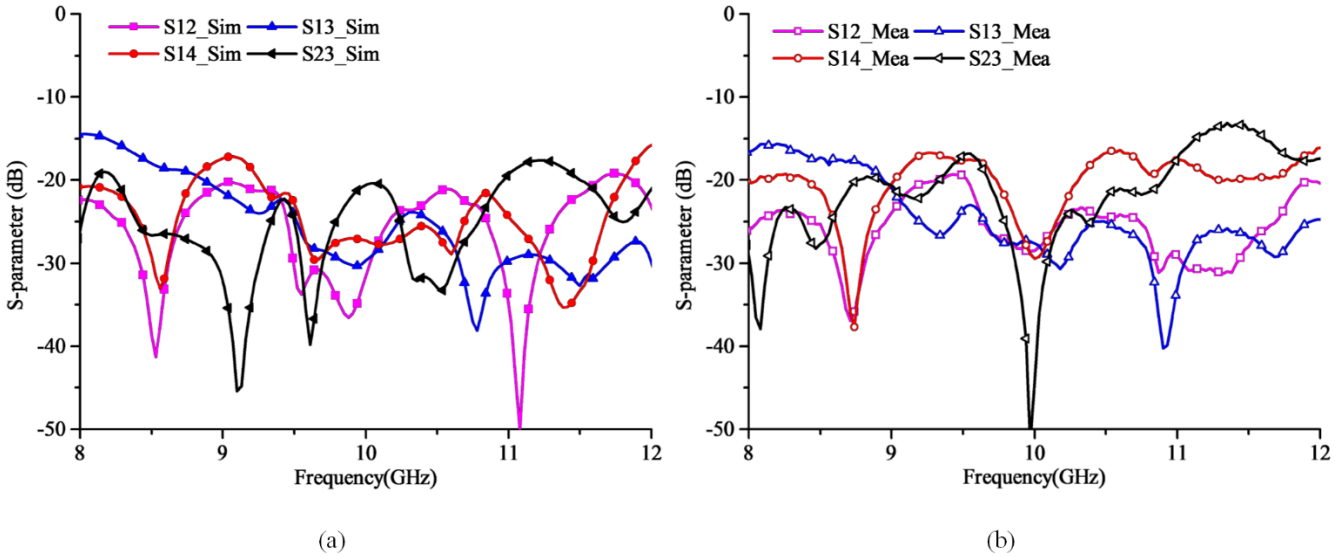

FIGURE 7. The isolations of beam ports. (a) Simulations, (b) Measurements.

lower band or higher band with the increase or decrease of the slot length *Ls*. The slot width *Ws* affects the impedance matching within the operation band. As expected, the slot width and length correspond to the characteristic impedance and electrical length of the transitions in the power dividers, respectively. The final detail parameters of the lens ports are list in Table 1. From the current propagating in Fig.2(d), the wave energy from beam ports B2 propagates along lens body to the array ports uniformly.

The return losses of beam ports B2 of these different Rotman lens are shown in Fig.4. The Rotman lens with triangular transitions which have gradual width changes shows a good return loss as expected in [14]. Whereas, the truncated ports have a width saltation so the impedance is very mismatched as shown in Fig.4. The Rotman lens with power dividers creates

TABLE 1. Detail parameters of lens ports. (Unit: mm).

Ports	B1	B2	A1	A2	A3	A4	D1	D2	D3
Wa	11.4	11.4	9.4	8.9	8.6	8.6	9.6	9.5	9.5
La	2.6	2.8	2.4	2.7	2.9	3.1	2.4	2.4	2.4
Ws	6.7	7.1	6.2	5.7	5.7	5.7	5.5	5.5	5.1
Ls	0.5	0.5	0.6	0.6	0.6	0.6	0.6	0.6	0.6
ds	0.9	1.2	0.5	0.8	1	1.2	0.5	0.5	0.5

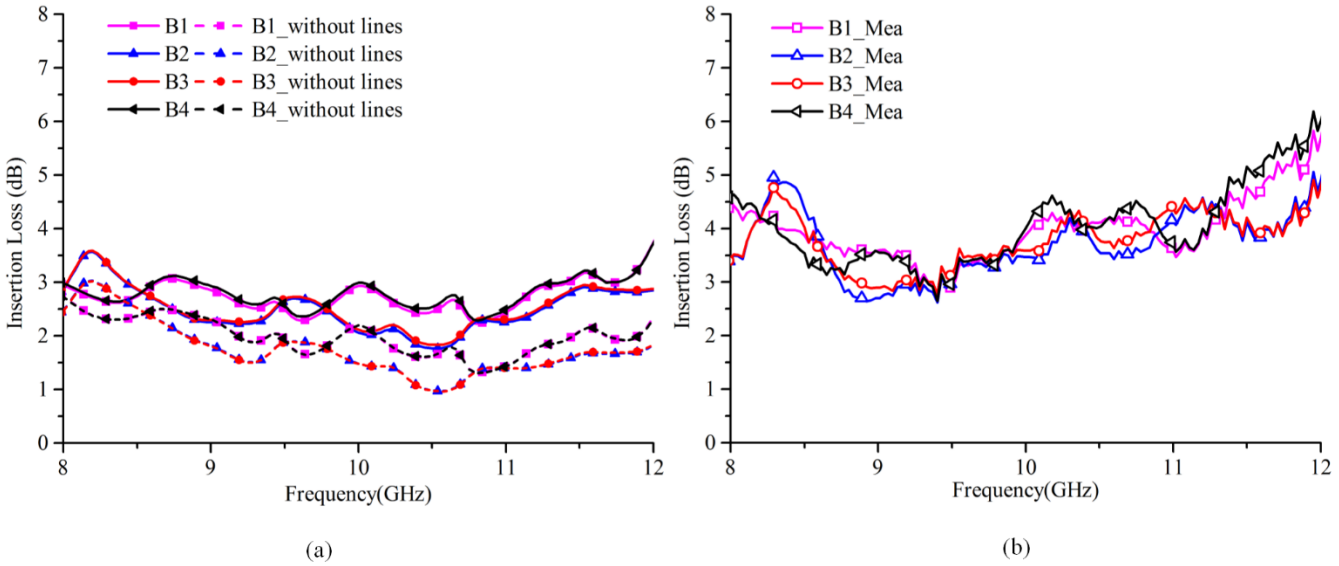

FIGURE 8. The insertion losses of beam ports. (a) Simulations, (b) Measurements.

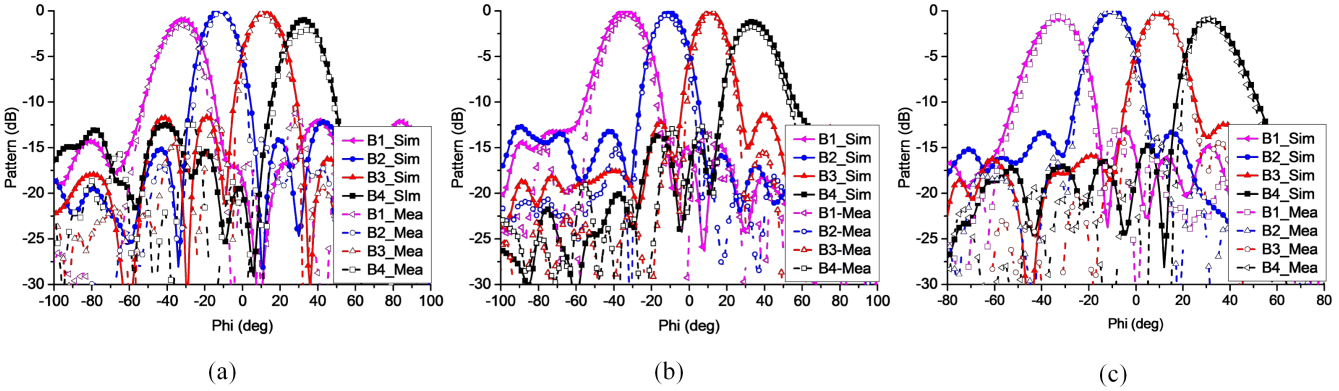

FIGURE 9. The simulated and measured normalized radiation patterns. (a) 9GHz, (b) 10GHz, (c) 11GHz.

a transition process for the wave energy propagating from the feed lines, so it realizes better impedance matching compared with the Rotman lens with truncated ports. The Rotman lens with rectangular energy distribution slots also realize impedance matching though its bandwidth is not wider than its predecessor due to its more compacter layout.

IV. SIMULATION AND MEASUREMENT RESULTS

A 4 × 7 Rotman lens using truncated ports with rectangular energy distribution slots is designed and prototyped at 10GHz to validate the proposed design. The prototypes are shown in Fig.5. The prototypes are tested for the purpose of demonstration. The simulated and measured results are given in detail.

The low return loss of the beam ports would ensure that as much as power would be emanated from the specific beam port to the array ports apertures. The simulated and measured results of |S11| of four beam ports are shown in Fig.6. The slight results variation may be caused by the insufficient machining accuracy. The Rotman lens exhibits a 27% bandwidth from 8.73 GHz to 11.42 GHz for VSWR < 2, which indicates that the ports with energy distribution slots realizes good match between the lens body and feed lines.

The simulated and measured isolations between the beam ports are shown in Fig.7. The Rotman lens is symmetrical, so only S12, S13, S14 and S23 are provided for conciseness. The results show that the isolations between the beam ports are better than 17.2 dB within the operation bandwidth.

The simulated and measured insertion losses from the beam ports to the array ports are shown in Fig.8. During the test, all ports except the tested ones were connected by high-performance SMA connectors. To guarantee enough distance between the SMA connectors for measurement, long feed lines and delay lines are used, which leads to about 0.58dB and 0.74dB loss for port B1 and port B2 at 10GHz, respectively. After the insertion losses of long feed lines and

TABLE 2. Comparison between this work and several Rotman Lenses.

Ref.	Ports Number (BP×AP)	Size	Number of Layers	Bandwidth
[10]	5×15	$17.9\lambda g \times 10.7\lambda g$	2	4.1%
[11]	6×8	$15.9\lambda g \times 5.6\lambda g$	2	14.3%
[14]	5×5	$6.2\lambda g \times 4.1\lambda g$	1	7.0%
This work	4×7	$4.8\lambda g \times 3.3\lambda g$	1	26.9%

delay lines being deducted, the simulated insertion losses of the Rotman lens are also shown in Fig.8. It can be seen that the proposed Rotman lens has low insertion losses of 2.19dB and 1.48dB at 10 GHz when B1 and B2 are excited, respectively. Compared with the simulation results, the measurement insertion losses are higher in high frequency band, which may be caused by the limited bandwidth performance of the real SMA connectors.

A broadband printed-dipole array [17] is connected to the Rotman lens through the delay lines for the purpose of demonstration as shown in Fig.5. The simulated and measured normalized radiation patterns at 9GHz, 10 GHz, 11 GHz are plotted in Fig. 9 for 4 beam ports. A good agreement between simulations and measurements is obtained. The beam scanning from $-33°$ to $33°$ in $11°$ increments is achieved. As expected, the directions of the scan angles remain unchanged since the Rotman lens is a true-time-delay beam former.

The size and the performance of the proposed Rotman lens are compared in Table 2 with related published Rotman lens in the literatures [10], [11], [14]. It shows that the proposed Rotman lens leads to a size reduction and has advantages of easy processing, wide bandwidth and low cost compared to other Rotman lens.

V. CONCLUSION

A compact printed Rotman lens with rectangular slotted ports is presented in this paper. The rectangular slotted ports are evolved from 1-2 power dividers. By using the proposed rectangular slotted ports, the size of the Rotman lens is miniaturized effectively without degrading its performance and increasing its cost of production. To validate the proposed design, a 4×7 compact Rotman lens with rectangular slotted ports is designed and prototyped at 10GHz. The Rotman lens can realize scanning range of $\pm 33°$. Besides, 27% bandwidth for VSWR < 2, the isolation between beam ports better than 17.2 dB, low insertion losses of 2.19dB and 1.48dB at 10 GHz are obtained when B1 and B2 are excited. Consequently, the advantages of compact size, low cost, convenient processing and wide bandwidth make the proposed Rotman lens a good candidate for the multi-beam antenna systems.

REFERENCES

[1] W. Lee, J. Kim, C. S. Cho, and Y. J. Yoon, "Beamforming lens antenna on a high resistivity silicon wafer for 60 GHz WPAN," *IEEE Trans. Antennas Propag.*, vol. 58, no. 3, pp. 706–713, Mar. 2010.
[2] Y. M. Cheng, P. Chen, W. Hong, T. Djerafi, and K. Wu, "Substrate-integrated-waveguide beamforming networks and multibeam antenna arrays for low-cost satellite and mobile systems," *IEEE Antennas Propag. Mag.*, vol. 53, no. 6, pp. 18–30, Dec. 2011.
[3] M. Rajabalian and B. Zakeri, "Optimisation and implementation for a non-focal Rotman lens design," *IET Microw. Antennas Propag.*, vol. 9, no. 9, pp. 982–987, Jun. 2015.
[4] W. Rotman and R. F. Turner, "Wide-angle microwave lens for line source applications," *IEEE Trans. Antennas Propag.*, vol. AP-11, no. 6, pp. 623–632, Nov. 1963.
[5] L. Schulwitz and A. Mortazawi, "A new low loss Rotman lens design using a graded dielectric substrate," *IEEE Trans. Microw. Theory Techn.*, vol. 56, no. 12, pp. 2734–2741, Dec. 2008.
[6] A. Ibbotson, D. I. L. de Villiers, and K. D. Palmer, "A defocused rotman lens with reduced conjugate port coupling," *IEEE Microw. Wireless Compon. Lett.*, vol. 23, no. 8, pp. 394–396, Aug. 2013.
[7] A. Darvazehban, O. Manoochehri, M. A. Salari, P. Dehkhoda, and A. Tavakoli, "Ultra-wideband scanning antenna array with rotman lens," *IEEE Trans. Microw. Theory Techn.*, vol. 65, no. 9, pp. 3435–3442, Sep. 2017.
[8] W. Lee, J. Kim, and Y. J. Yoon, "Compact two-layer rotman lens-fed microstrip antenna array at 24 GHz," *IEEE Trans. Antennas Propag.*, vol. 59, no. 2, pp. 460–466, Feb. 2011.
[9] K. T. V. Dai, T. Nguyen, and O. Kilic, "A compact microstrip rotman lens design," in *Proc. United States Nat. Committee URSI Nat. Radio Sci. Meeting (USNC-URSI NRSM)*, Boulder, CO, USA, Jan. 2017, pp. 1–2.
[10] K. Tekkouk, M. Ettorre, L. Le Coq, and R. Sauleau, "Multibeam SIW slotted waveguide antenna system fed by a compact dual-layer rotman lens," *IEEE Trans. Antennas Propag.*, vol. 64, no. 2, pp. 504–514, Feb. 2016.
[11] Y. Liu, H. Yang, Z. Jin, F. Zhao, and J. Zhu, "Compact Rotman lens-fed slot array antenna with low sidelobes," *IET Microw., Antennas Propag.*, vol. 12, no. 5, pp. 656–661, Apr. 2018.
[12] T. K. V. Dai and O. Kilic, "Compact Rotman lens structure configurations to support millimeter wave devices," *Prog. Electromagn. Res. B*, vol. 71, pp. 91–106, Aug. 2016.
[13] R. C. Hansen, "Design trades for Rotman lenses," *IEEE Trans. Antennas Propag.*, vol. 39, no. 4, pp. 464–472, Apr. 1991.
[14] L. Musa and M. S. Smith, "Microstrip port design and sidewall absorption for printed Rotman lenses," *IEE Proc. H-Microw., Antennas Propag.*, vol. 136, no. 1, pp. 53–59, Feb. 1989.
[15] A. Attaran, R. Rashidzadeh, and A. Kouki, "60 GHz low phase error Rotman lens combined with wideband microstrip antenna array using LTCC technology," *IEEE Trans. Antennas Propag.*, vol. 64, no. 12, pp. 5172–5180, Dec. 2016.
[16] Q. Liang, G. Zhou, B. Sun, and J. Li, "Compact microstrip rotman lens using Chebyshev impedance transformers," *Progr. Electromagn. Res. Lett.*, vol. 76, pp. 1–6, Apr. 2018.
[17] S. X. Ta, H. Choo, and I. Park, "Broadband printed-dipole antenna and its arrays for 5G applications," *IEEE Antennas Wireless Propag. Lett.*, vol. 16, pp. 2183–2186, 2017.

QIUYAN LIANG was born in Shanxi, China, in 1993. She received the B.Eng. degree from the North University of China, Taiyuan, China, in 2014. She is currently pursuing the Ph.D. degree in electromagnetic field and microwave technology with Xidian University. Her research interests include the multi-beam antenna systems and beam steering antenna.

BAOHUA SUN was born in Hebei, China, in 1969. He received the B.Eng. degree in radio electronic from Hebei University, Baoding, China, in 1992, and the M.Eng. and Ph.D. degrees in electromagnetic and microwave technology from Xidian University, Xi'an, China, in 1996 and 2000, respectively. From 2000 to 2003, he was a Postdoctoral Research Associate with Amoi Corporation, Xiamen, China. In 2003, he joined the National Key Laboratory of Antennas and Microwave Technology, Xidian University, where he is currently a Professor. His current research interests include broadband and miniaturized antennas, broadband antenna arrays, nonfoster active antennas, mm-wave antennas, and RF circuits.

GAONAN ZHOU was born in Fujian, China, in 1992. He received the B.Eng. degree from the Huaihai Institute of Technology, Lianyungang, China, in 2015. He is currently pursuing the M.S. degree in electromagnetic field and microwave technology with Xidian University. His research interests include the multi-beam feed networks and high gain antenna.

JIANPING ZHAO received the B.Sc. degree in applied physics and the M.Eng. degree in signal and information processing from Xidian University, Xi'an, China, in 1991 and 1996, respectively, and the Ph.D. degree in signal and information processing from the Beijing University of Posts and Telecommunications, Beijing, China, in 1999. From 1999 to 2008, he was the Chief Engineer with the Research and Develop Centre, Zhongxing Telecommunication Equipment Corporation, Xi'an. Since 2008, he has been the Chief Expert with the Antenna and System Technology Centre, Huawei Technologies Company, Ltd., Shanghai, China, where he is also a Senior Engineer. His current research interests include multi-in multi-out, radio frequency circuit design, and signal processing. He has taken the leadership of several national science and technology major projects, including National 863 and 973 Programs.

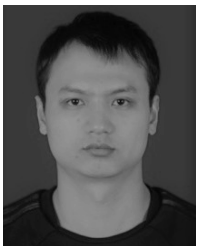

GUANXI ZHANG received the B.S. and Ph.D. degrees from Xidian University, Xi'an, in 2011 and 2016, respectively. He is currently with Huawei Technologies Company, Ltd. His current research interests include 5G communications, beam-forming networks, and array antenna synthesis.